NUMERICAL MODELING OF ELECTRIC FIELD DISTRIBUTION IN SUBCUTANEOUS TUMORS TREATED WITH NEEDLE ELECTRODES

Selma Čorović[1] and Damijan Miklavčič[1]

[1]University of Ljubljana, Faculty of Electrical Engineering,
1000 Ljubljana, Tržaška 25, Slovenia

selma.corovic@fe.uni-lj.si (Selma Čorović)

Abstract

Electrochemotherapy (ECT) is an effective antitumor treatment employing locally applied high electric pulses in combination with chemotherapeutic drugs. As a response to the high electric pulses delivery, a local electric field (E) is established within the treated tissue. The antitumor treatment outcome is directly related to the electric field distribution over the tumor tissue. For successful therapy the entire tumor tissue needs to be subjected to the local electric field strength above the reversible threshold E_{rev}. This value is the critical reversible threshold value of the local electric field (E_{rev}) which causes structural changes in the target tissue. Namely, it initializes electropermeabilization of cell membranes, which allows for increased entrance of the drug into the cell and thus allows for improved effectiveness of chemotherapy. The local electric field distribution depends on parameters of electric pulses delivered through electrodes to the treated tissue, the shape and position of the electrodes with respect to the treated tissue, as well as the structure of the tumor and its surrounding tissue. The objective of this study is to calculate and compare the local electric field distribution in the 3D numerical model of subcutaneous tumor obtained with needle electrodes by means of finite element method. We demonstrate that by appropriate number, depth of insertion and arrangement of electrodes as well as amplitude of electric pulses a better coverage by sufficiently high electric field ($E \geq E_{rev}$) can be achieved over the entire target tissue (i.e. the tumor) while being minimized in the surrounding healthy tissues.

Keywords: electropermeabilisation, electrochemotherapy, finite element method, subcutaneous tumor, needle electrodes.

Author's biography

Selma Čorović received the B.A.Sc. and M.Sc. degrees in electrical engineering from the University of Ljubljana, Ljubljana, Slovenia. Currently, she is Assistant Researcher at the University of Ljubljana. Her main research interest is in the field of numerical modeling of electric field distribution in biological tissue, experimental work on visualization of electropermeabilization process *in vivo* and development of web-based e-learning applications aimed at providing the knowledge on electropermeabilization of biological tissues.

1 Introduction

Electrochemotherapy (ECT) is an effective approach in tumor treatment employing locally applied high-voltage electric pulses (HV pulses) in combination with chemotherapeutic drugs. The ECT is performed using either intravenous or intratumoral drug injection, followed by application of electric pulses, generated by an electric pulses generator and delivered to the target tissue via appropriate electrodes. As a response to the high electric pulses delivery, a local electric field (E) is established within the treated tissue. A sufficient magnitude of electric field initializes electropermeabilization of cell membranes, which allows for increased entrance of the drug into the cell and thus allows for improved effectiveness of chemotherapy. This value is the critical reversible threshold value of the local electric field (E_{rev}) which causes structural changes in the target tissue. Namely, when E_{rev} is achieved, cell membranes are being permeabilizated and chemotherapeutic drugs enter the target cells. Such a modality of cell membrane permeabilization by means of electric field is named electropermeabilization [1].

For successful electrochemotherapy the entire volume of the target/tumor tissue need to be subjected to the local electric field above reversible threshold value (E_{rev}). By appropriate selection of electrodes and amplitude of electric pulses the needed electric field can be obtained only inside the target/tumor tissue, while the damage to the surrounding healthy tissue is prevented or minimized. The needed parameters for each individual type of tumor can be determined, and thus the needed treatment planning carried out, by means of numerical modeling [2].

In our present study we calculated and compared local electric field distribution inside the numerical model of subcutaneous tumor for four different needle electrode configurations usually used in clinics and research [1,2,3,4]. Our objective was to investigate the influence of number, depth of insertion and arrangement of needle electrodes as well as amplitude of electric pulses on the local electric field distribution inside the model of subcutaneous tumor with homogeneous and non-homogeneous electrical properties.
Based on numerical results we determined the appropriate electrode configuration for the given geometry and electrical properties of subcutaneous tumor in a way that the entire volume of the tumor was subjected to the sufficiently high electric field ($E \geq E_{rev}$) and minimized in the surrounding tissues.

2 Numerical modeling

The 3D models are based on the numerical solution of partial differential equations for steady electric current in isotropic conductive media. The numerical calculations were performed by means of finite element method using FEMLAB software package Femlab (3.0) [Femlab 2001] in the *3D* Conductive Media DC application mode. With no applied current source, this mode solves Laplace's equation (Eq. (1)):

$$-\nabla \cdot (\sigma \cdot \nabla \varphi) = 0\,, \qquad (1)$$

where σ and φ indicate tissue conductivity and electric potential, respectively. All the simulations were run on a PC running Windows 2000 with a 2.6 GHz Pentium 4 processor and 1 GB of RAM.

2.1 Tissue geometry definition and electrodes modeling

The model of a subcutaneous tumor treated with electrochemotherapy consists of two tissues, the tumor tissue, which is the target tissue, and its surrounding tissue. The input to the model is the constant voltage applied to the electrodes and corresponds to the amplitude of the electroporation pulses generated by the high voltage generator. The output of the model is the electric field distribution inside the target tissue (e.g. cutaneous tumor). The tumor tissue was modeled as a sphere with 2 mm diameter. The 3D geometry of subcutaneous tumor is shown in Fig. 1, where σ_2 and σ_1 indicate

specific conductivities of tumor tissue and its surrounding tissue, respectively.

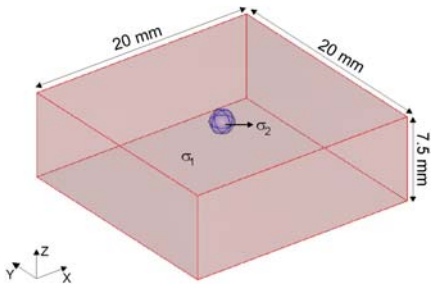

Fig. 1 3D geometry of subcutaneous tumor, where σ_2 and σ_1 indicate specific conductivities of tumor tissue and the surrounding tissue, respectively.

The 3D model of subcutaneous tumor with electrodes configurations, studied in this paper, are shown in Figs. 2a, 2b and 2c.

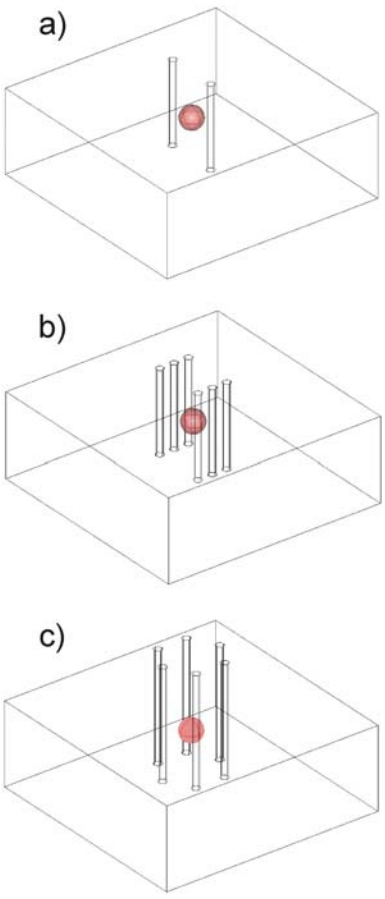

Fig. 2 3D geometries of subcutaneous tumor with three needle electrode configurations: a) one-needle pair; b) three-needle pairs and six-needle array.

Electric field distribution in the model of subcutaneous tumor treated with one-needle pair and three-needle pairs electrode configurations was studied for two different depth of electrode' insertion: ℓ = 5mm and ℓ = 3 mm. In subcutaneous tumor model treated with six-needle array electrode configuration the electric field distribution was studied only for ℓ = 3 mm. The 2D geometry of the models is shown in Fig. 3.

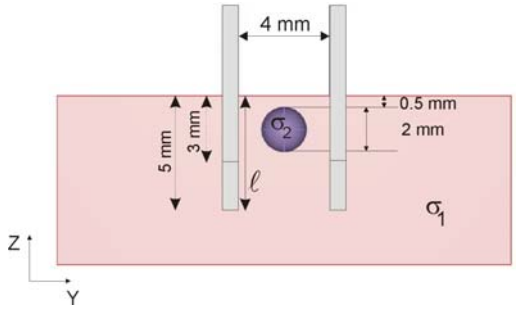

Fig. 3 2D geomertry of subcutaneous tumor model in the central YZ plane, where ℓ indicates the depth of insertion of needle electrodes.

The Fig. 4 illustrates the electrode configurations with their respective dimensions, arrangement and polarities electrode geometry for one-needle (Fig. 4 a) and three-needle pairs of electrodes (Fig. 4b) and six-needle array with two distinct polarities: 2×2 array (Fig. 4c) and 3×3 (Fig. 4d).

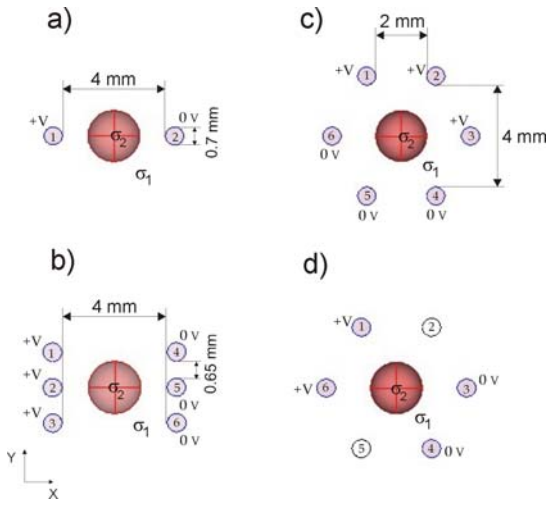

Fig. 4 Electrode configurations with their respective dimensions, arrangement and polarities: a) one-needle pair; b) three-needle pairs; 2×2 six-needle array and d) 3×3 six needle array.

2.2 Boundary conditions

The voltage delivered to the tissue from the electric pulses generator was modeled as a constant potential set to the surface of the electrodes. Based on this the Direchlet boundary condition was defined. The Neumann boundary condition, i.e. the electric-insulation condition was set to the rest of the outer boundaries of the models specifying that no current flows across the boundaries. The continuity condition is automatically set on the interior boundaries specifying that the normal components of the electric current across the boundary between the surrounding tissue and the tumor are continuous.

2.3 Electrical properties of the modeled tissues

The tumor and surrounding tissue inside the model are considered conductive materials where current flows due to the applied electric field. Electrical properties of the tissues in the model are characterized by their specific conductivities according to published data in the literature [5]. The conductivities set to the region in the model representing tumor tissue were 0.2 S/m and 0.4 S/m, while the conductivity of the region representing the surrounding tissue was set to be 0.2 S/m. Both tissues are considered to be isotropic and homogeneous. The value 0.4 S/m represents the conductivity of unpermeabilised tumor tissue, while the value 0.2 S/m describes the conductivity of the layers composing the surrounding skin tissue, not considering the resistance of the stratum corneum that is almost immediately broken at the beginning of the first pulse.

2.4 Threshold values E_{rev} and E_{irrev} definition

Electropermeabilisation of the cell membrane, i.e. a process of increasing cell membrane permeability occurs when the local electric field strength *(E)* within the treated tissue exceeds the reversible threshold value E_{rev}. The electropermeabilisation of the tissue ($E \geq E_{rev}$) is reversible and the viability of the cells inside the treated tissue is not affected until the local electric field strength exceeds the irreversible threshold value ($E \geq E_{irrev}$). The critical values E_{rev} and E_{irrev} are characteristic for each type of tissue and depend on the structure of the particular tissue (i.e. cell size, shape, distribution, orientation…). In our models the electric field distribution is displayed in the range from E_{rev} = 400 V/cm to E_{irrev} = 900 V/cm. These values (E_{rev} and E_{irrev}) have been previously determined based on *in vivo* measurements and numerical modeling and published by [5].

3 Results

In electrochemotherapy it is necessary that the electric field inside the entire target tissue exceeds reversible threshold E_{rev}. In order to meet this condition we calculated the needed voltage (i.e. critical voltage *Uc*) for each electrode configuration in a way that the minimum electric field (Et_{min}) within the entire volume of the target tissue exceeds $Et_{min} \geq 400\ V/cm$ (see Table 1).

The critical voltage *Uc* and the corresponding electric current *I* was calculated for two different electrical properties of subcutaneous tumor. In the first case the specific conductivitiy of the tumor tissue was 0.2 S/m (σ_2 = 0.2 S/m) and in the second case the tumor tissue was 0.4 S/m (σ_2 = 0.4 S/m). The calculated values of *Uc* and *I* for each electrode configuration, given in Fig. 4, are listed in Table 1.

ISBN 978-3-901608-32-2

Tab. 1 The critical voltage *Uc* and the electric current *I* for given electrodes' configurations

Electrode configuration	ℓ mm	σ S/m	Uc V	I A
Fig. 4a 1-needle pair	5	$\sigma_2=\sigma_1$	300	0.354
	3	$\sigma_2=\sigma_1$	330	0.264
	5	$\sigma_2=2\sigma_1$	380	0.454
	3	$\sigma_2=2\sigma_1$	430	0.349
Fig. 4b 3-needle pairs	5	$\sigma_2=\sigma_1$	200	0.319
	3	$\sigma_2=\sigma_1$	220	0.308
	5	$\sigma_2=2\sigma_1$	260	0.420
	3	$\sigma_2=2\sigma_1$	290	0.412
Fig. 4c 2x2 six-needle array	3	$\sigma_2=\sigma_1$	230	0.466
	3	$\sigma_2=2\sigma_1$	350	0.411
Fig. 4d 3x3 six-needle array	3	$\sigma_2=\sigma_1$	265	0.336
	3	$\sigma_2=2\sigma_1$	310	0.572

Based on numerical analysis of electric field distribution we found that the most appropriate electrode configuration for the given geometry and electrical properties of subcutaneous tumor was the three-needle pairs of electrodes (Fig. 4b) with depth of electrode' insertion ℓ = 3 mm. The needed voltage *Uc* for the homogeneous ($\sigma_2 = \sigma_1$) and for non-homogeneous ($\sigma_2 = 2\sigma_1$) model was Uc = 220 V and Uc = 290 V, respectively, (see Table 1).

In order to compare the results obtained with the three-needle pairs of electrodes (Fig. 4b) to the results obtained with one-needle pair, 2×2 and 3×3-nedle array of electrodes we calculated the electric field distribution for the same voltage Uc = 290 V within the non-homogeneous model of subcutaneous tumor ($\sigma_2 = 2\sigma_1$, $\sigma_1 = 0.2$ S/m; $\sigma_2 = 0.4$ S/m).

In Fig. 6, the electric field distribution obtained with one-needle pair of electrodes and two electrodes' depth of insertion (3 and 5 mm) is shown in XY, YZ and XZ cross-sections planes.

In Fig. 7, the electric field distribution obtained with three-needle pair of electrodes and two electrodes' depth of insertion (3 and 5 mm) is shown in XY, YZ and XZ cross-sections planes.

In Fig. 8 and Fig. 9, the electric field distribution obtained with 2×2 and 3×3 six-needle array of electrodes is shown, respectively, in XY, YZ and XZ cross-sections planes. The electrodes' depth of insertion was 3 mm for both configurations.

Values of electric field strength are displayed in the range $E_{rev} \le E \le E_{irrev}$ (E_{rev} = 400 V/cm, E_{irrev} = 900 V/cm), as shown in Fig. 5. The white region ($E \ge E_{rev}$) represents insufficiently electropermeabilised regions of tissue and the patterned region represents irreversibly electropermeabilised regions of tissue ($E \ge E_{irrev}$).

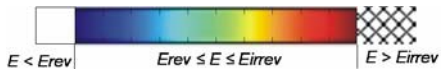

Fig. 5 The color legend showing electric field strength in the range *Erev* ≤ *E* ≤ *Eirrev*. (*Erev* = 400 V/cm, *Eirrev* = 900 V/cm)

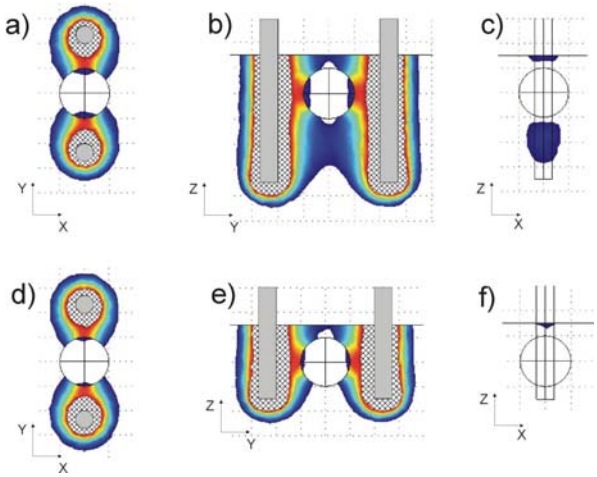

Fig. 6 Electric field distribution around one-needle pair of electrodes in three central perpendicular planes: a) XY, b) YZ and c) XZ in the model with depth of electrodes' insertion ℓ= 5 mm and d) XY, e) YZ and f) XZ in the model with depth of electrodes' insertion ℓ= 3 mm. Voltage applied was 290 V.

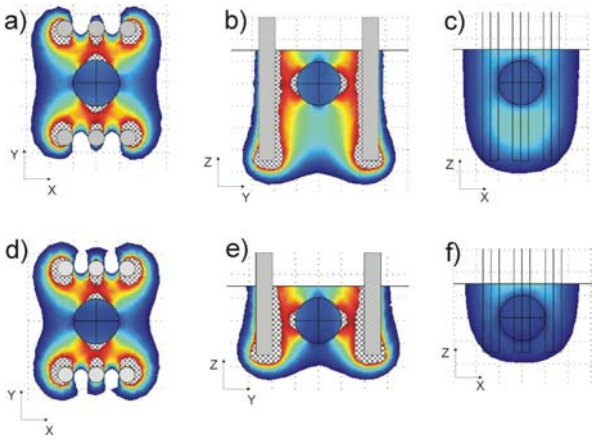

Fig. 7 Electric field distribution around three-needle pairs of electrodes in three central perpendicular planes: a) XY, b) YZ and c) XZ in the model with depth of electrodes' insertion ℓ= 5 mm and d) XY, e) YZ and f) XZ in the model with depth of electrodes' insertion ℓ= 3 mm. Voltage applied was 290 V.

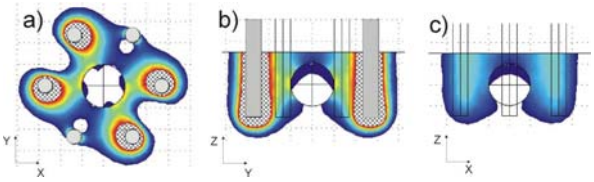

Fig. 8 Electric field distribution around 2x2 six-needle array electrodes in three central perpendicular planes: a) XY, b) YZ and c) XZ in the model with depth of electrodes' insertion ℓ= 3 mm. Voltage applied was 290 V.

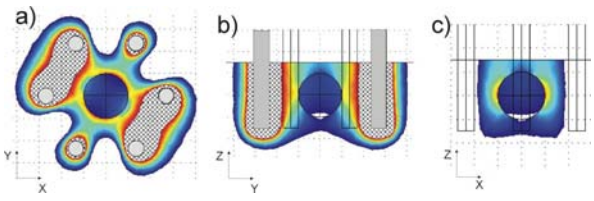

Fig. 9 Electric field distribution around 3x3 six-needle array electrodes in three central perpendicular planes: a) XY, b) YZ and c) XZ in the model with depth of electrodes' insertion ℓ= 3 mm. Voltage applied was 290 V.

4 Discussions and conclusions

The objective of this study was to calculate and compare the local electric field distribution in the 3D numerical model of subcutaneous tumor obtained with four different configurations of needle electrodes by means of finite element method. We showed that the local electric field distribution depends on the number, arrangement, depth of electrodes' insertion, the amplitude of electric pulses, as well as the specific conductivities of the tumor and its surrounding tissue. We demonstrated that by appropriate number, depth of insertion and arrangement of electrodes as well as amplitude of electric pulses the appropriate coverage by sufficiently high electric field ($E \geq E_{rev}$) can be achieved over the entire target tissue (i.e. the tumor) and minimized in the surrounding tissues.

5 References

[1] D. Miklavčič, D. Šemrov, H. Mekid, and L. M. Mir. A validated model of in vivo electric field distribution in tissues for electrochemotherapy and for DNA electrotransfer for gene therapy. *Biochimica et Biophysica Acta*, 1523: 73-83, 2000.

[2] D. Miklavčič, S. Čorović, G. Pucihar, and N. Pavšelj. Importance of tumor coverage by sufficiently high local electric field for effective electrochemotherapy. *EJC Supplements,* 4: 45-51, 2006.

[3] D. Šel, S. Mazeres, J. Teissie and D. Miklavčič. Finite-element modeling of needle electrodes in tissue from the perspective of frequent model computation. *IEEE transactions on biomedical engineering*, 50: 1221-1231, 2003.

[4] R. Gilbert, M. Jaroszeski, and R. Heller. Novel electrode designs for electrochemotherapy. *Biochim. Biophis. Acta,* 1334: 9-14, 1997.

[5] N. Pavšelj, Z. Bregar, D. Cukjati, D. Batiuskaite, L. M. Mir, and D. Miklavčič. The course of tissue permeabilization studied on a mathematical model of a subcutaneous tumor in small animals. *IEEE Trans. Biomed. Eng*, 52: 1373-1381, 2005.

